

# Fitness Costs of Antibiotic Resistance Impede the Evolution of Resistance to Other Antibiotics

Farhan R. Chowdhury and Brandon L. Findlay\*

Cite This: <https://doi.org/10.1021/acsinfecdis.3c00156>

Read Online

ACCESS |



Metrics &amp; More



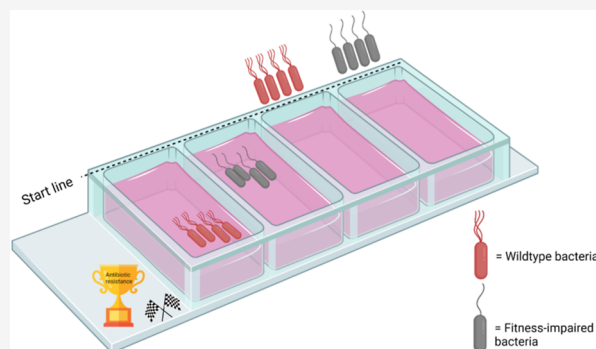
Article Recommendations



Supporting Information

**ABSTRACT:** Antibiotic resistance is a major threat to global health, claiming the lives of millions every year. With a nearly dry antibiotic development pipeline, novel strategies are urgently needed to combat resistant pathogens. One emerging strategy is the use of sequential antibiotic therapy, postulated to reduce the rate at which antibiotic resistance evolves. Here, we use the soft agar gradient evolution (SAGE) system to carry out high-throughput in vitro bacterial evolution against antibiotic pressure. We find that evolution of resistance to the antibiotic chloramphenicol (CHL) severely affects bacterial fitness, slowing the rate at which resistance to the antibiotics nitrofurantoin and streptomycin emerges. In vitro acquisition of compensatory mutations in the CHL-resistant cells markedly improves fitness and nitrofurantoin adaptation rates but fails to restore rates to wild-type levels against streptomycin. Genome sequencing reveals distinct evolutionary paths to resistance in fitness-impaired populations, suggesting resistance trade-offs in favor of mitigation of fitness costs. We show that the speed of bacterial fronts in SAGE plates is a reliable indicator of adaptation rates and evolutionary trajectories to resistance. Identification of antibiotics whose mutational resistance mechanisms confer stable impairments may help clinicians prescribe sequential antibiotic therapies that are less prone to resistance evolution.

**KEYWORDS:** antibiotic resistance, fitness costs, soft agar gradient evolution, sequential antibiotic therapy, efflux



The rapid rise of antibiotic resistance severely burdens healthcare systems worldwide, increasing hospital stays and causing increased mortality. A recent study has estimated that infections caused by antibiotic-resistant pathogens directly led to 1.2 million premature deaths in 2019 alone.<sup>1</sup> If the current increase in the incidence of these infections continues, the WHO estimates that resistant pathogens could kill 10 million people and cause more than \$1 trillion in losses annually by the year 2050.<sup>2,3</sup>

The current antibiotic resistance crisis is driven by a combination of the incredible speed at which bacteria can evolve resistance and a myriad of other factors related to antibiotic stewardship, including inadequate drug regulations and the widespread use of antibiotics in livestock.<sup>4,5</sup> Critically, the development of new antibiotics has not kept pace with the spread of resistance mechanisms: only eight new antibiotics have been approved since 2017, most of which are derivatives of existing antibiotics.<sup>6</sup> To maintain the effectiveness of our current therapies, we urgently need to develop new strategies to combat antibiotic-resistant pathogens and the evolution of resistance itself.

Evolutionary strategies to combat resistance evolution have gained attention in recent years.<sup>7</sup> The evolution of resistance often incurs a fitness cost to the bacteria, from increased sensitivity to abiotic stressors, to reduced growth rates and

motility.<sup>8–10</sup> Reduced growth and movement rates impede the ability of bacterial populations to acquire nutrients and move away from toxic compounds,<sup>8</sup> while reduced fitness can hinder individual mutants' ability to compete with fitter cells that exhibit lower resistance levels.<sup>9,10</sup> However, prolonged antibiotic therapies during the treatment of cystic fibrosis, chronic liver disease, and respiratory infections, and recurring urinary tract infections can clear wild-type (WT) or low-level resistant populations completely, eliminating competition for resistant cells.<sup>11–14</sup> This necessitates switching therapy to a different antibiotic to continue effective treatment. Recent studies have highlighted strategies to optimize the design of sequential antibiotic therapy for improved infection clearance and limited resistance evolution.<sup>15–17</sup> Most of these studies leverage collateral sensitivity, a phenomenon where resistance to one drug induces hypersensitivity to another, to guide optimal antibiotic switches. However, collateral sensitivity is rare, and

Received: April 5, 2023

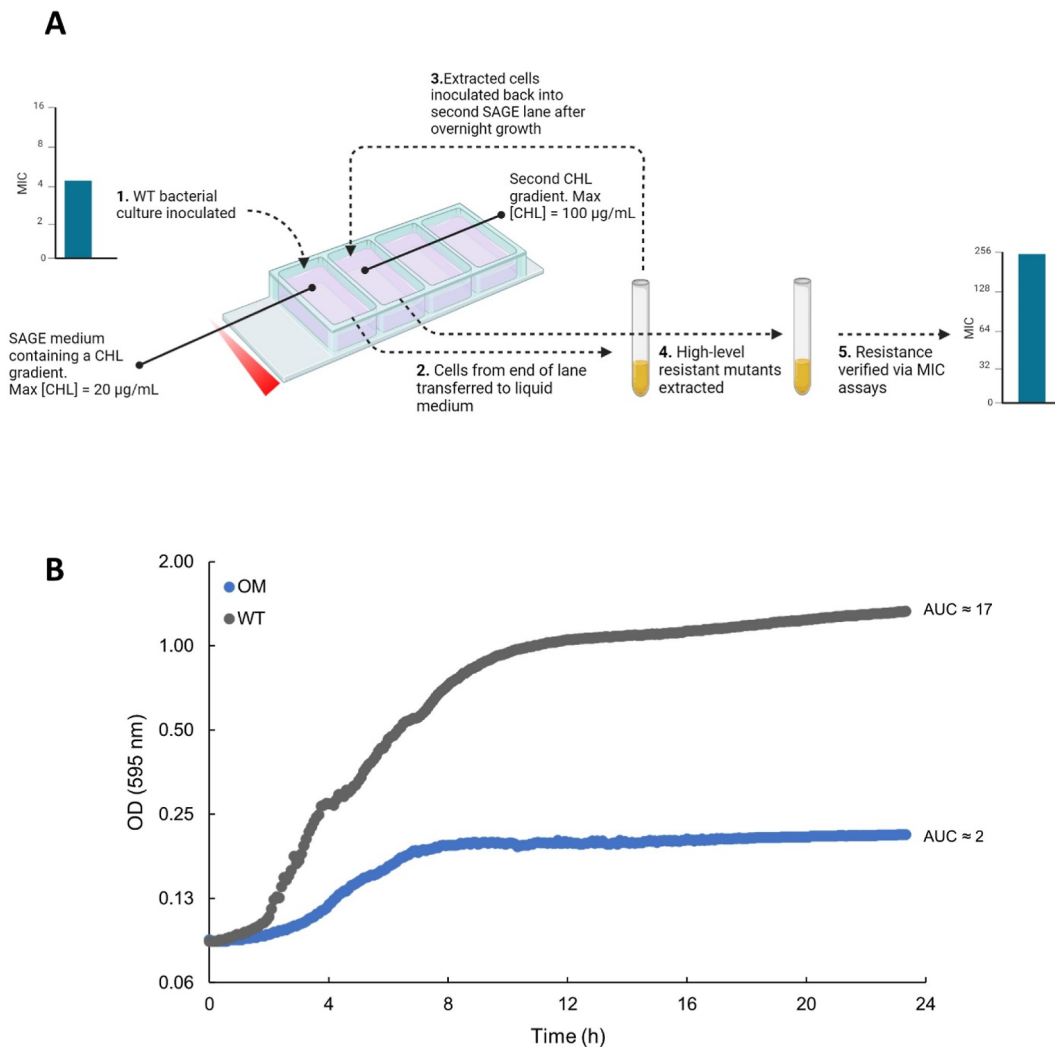


**Figure 1.** Evolution of CHL resistance incurs fitness costs. (A) Evolution of CHL resistance via the SAGE system. WT bacterial culture is inoculated in a CHL gradient (maximum [CHL] = 20  $\mu\text{g/mL}$ ) set up in soft-agar medium. Bacteria moving down a lane to access nutrients and space generate mutants that are able to resist the increasing concentrations of the antibiotic. When cells reach the end of a lane, they are extracted and cultured overnight and used to inoculate a new CHL gradient (maximum [CHL] = 100  $\mu\text{g/mL}$ ). Cells from the end of this secondary lane are extracted, and their resistance levels determined. Although depicted in the same plate, a new plate is used for each SAGE evolution cycle. (B) Growth curves of the WT and OM. Area under the curves (AUCs) show the OM to be heavily fitness impaired.

its application is limited by contradictory results on evolutionary repeatability and its generalizability across different genetic backgrounds.<sup>17–19</sup>

Hypersensitive bacterial populations are often growth-impaired, and Brepoels et al. recently showed that resistance evolution is impaired in hypersensitive bacterial populations independently of collateral sensitivity in certain drug sequences.<sup>20,21</sup> Here, we show that evolution of resistance to chloramphenicol (CHL) in *Escherichia coli* K-12 substrain MG1655 cripples its growth rate and movement through soft agar, which impedes its ability to evolve resistance to secondary antibiotics in antibiotic gradients independently of collateral sensitivity. We leveraged the high-throughput mutant generation capacity of the soft agar gradient evolution (SAGE) system to evolve 16 independent isogenic populations (referred to here as replicates) of WT and CHL-resistant *E. coli* (OM) separately to two different antibiotics, nitrofurantoin (NIT) and streptomycin (STR) in parallel.<sup>22</sup> By tracking distance moved in SAGE plates and observing growth patterns, we found that resistance was delayed by a day in the majority

of OM replicates. We then verified the role of fitness in the adaptation slowdown by evolving CHL-resistant mutants with improved growth and swim rates. These fitter mutants could restore WT-like adaptation rates to nitrofurantoin, but the slowdown in STR-adaptation persisted. Genome sequencing revealed divergent evolutionary trajectories across the differing genetic backgrounds, with fitness costs constraining the available paths to resistance. We suggest that these results are not tied to the primary antibiotic or the genetic background but to the fitness costs of resistance to the primary antibiotic. Consistent with this view, resistance is also impaired in a cefazolin (CFZ)-resistant mutant of *E. coli* BW25113. Our findings show that resistance mechanisms that incur heavy fitness penalties can serve as an indicator of subsequent evolution impairments which can shape primary antibiotic choices, and the SAGE system can be used to track in vitro evolutionary kinetics at high-throughput.

## RESULTS

**Evolution of High-Level Resistance to Chloramphenicol via SAGE.** We reported the evolution of resistance in *E. coli* MG1655 to a number of antibiotics representing different classes, including CHL, via the SAGE system before.<sup>22</sup> WT cells were passed through a SAGE plate containing a maximum [CHL] = 20  $\mu\text{g}/\text{mL}$  (WT MIC: 4  $\mu\text{g}/\text{mL}$ ) (Figure 1A). Cells extracted from the end of the plate were grown overnight and inoculated in a second SAGE plate containing a maximum [CHL] = 100  $\mu\text{g}/\text{mL}$ . Cells evolved from these plates exhibited CHL minimum inhibitory concentration (MIC) of 256  $\mu\text{g}/\text{mL}$ .

The WT *E. coli* MG1655 used in this study had 75 previously reported nonsynonymous mutations (Supporting Information) possibly acquired during the “speed-selection” process, which involves selecting for cells that move the quickest through SAGE medium.<sup>22</sup> The original CHL-resistant mutant (OM) acquired 54 nonsynonymous mutations distinct from the speed-selected *E. coli* MG1655 progenitor (Supporting Information), including mutations in multiple efflux-related genes like *acrB* (a component of the AcrAB-TolC efflux pump), *acrR* (the repressor of *acrAB*), *marR* (the multiple antibiotic resistance repressor, truncated in OM), *mprA/emrA* (repressor of the *marRAB* operon), and *rob* (transcriptional regulator of the *marA/soxS/rob* regulon involved in antibiotic resistance). All of these have been previously implicated in CHL resistance.<sup>23–26</sup> Upregulation of efflux systems is a common response to antibiotic stress in Gram-negative bacteria,<sup>27,28</sup> and efflux pumps are known to confer resistance to a wide range of antibiotic classes.<sup>29</sup> As expected, we found the OM to be resistant to many first-line agents susceptible to efflux (Table 1).

**Table 1. OM Exhibited a Multidrug-Resistant Phenotype**

antibiotic	class	MIC of WT ( $\mu\text{g}/\text{mL}$ )	MIC of OM ( $\mu\text{g}/\text{mL}$ )
amoxicillin	$\beta$ -lactam	4	16
ceftazidime	cephalosporin	$\leq 0.5$	4
cefazolin	cephalosporin	1	16
chloramphenicol	amphenicol	16	256
ciprofloxacin	fluoroquinolone	0.0156	4
tetracycline	tetracycline	1	64
tigecycline	tetracycline	$\leq 0.25$	2
trimethoprim	folic acid synthesis inhibitor	1	16

**Chloramphenicol-Resistant Cells Are Fitness Impaired.** We observed a slowdown in the movement of OM populations through antibiotic-free soft agar when compared to WT. While WT populations were able to traverse half the plate (40 mm) in  $\sim 6$  h, OM populations required  $\sim 24$  h to move the same distance (Movie S1). Movement through soft agar is dependent on bacterial growth: the faster cells grow, the quicker they populate and deplete resources from their surroundings, prompting movement to gain access to new space and nutrients via chemotaxis. While the WT quickly formed a high-density band of cells at the leading edge of growth, we observed a significant delay in the formation of this band by the OM (Movie S1). Comparing the speed of these bands showed the OM to be  $\sim 2$  times slower than the WT.

To link this reduction in movement through soft agar to fitness, we used the area under the curve (AUC) measure-

ments to quantify bacterial growth.<sup>20,30</sup> AUC incorporates three fitness parameters: the lag phase duration, the exponential growth rate, and the yield (maximum cell density). The AUC of the WT population was  $\sim 8$  times higher than that of the OM, showing large growth deficits (Figure 1B).

To confirm that accumulation of growth deficits is not a general outcome of SAGE experiments, we also analyzed growth curves for a NIT and a STR-resistant *E. coli* evolved in SAGE. AUCs of both mutants were similar to that of the WT (Figure S1). Correspondingly, resistance to STR did not significantly impede growth or movement in SAGE (Movie S1).

Efflux pumps are powered directly by the proton motive force and are energetically costly.<sup>31,32</sup> In addition to changes in efflux pumps, sequencing of the OM also revealed a truncation in the flagellar basal-body rod protein FlgG, which is essential for cell motility.<sup>33</sup> Cutting down on energetically expensive motility mechanisms may have allowed the mutant to direct more resources toward efflux and growth. A number of other mutations in genes related to metabolism, biosynthesis, the electron transport chain, and membrane transport were also identified in the OM, including a synonymous mutation in the chemotaxis protein CheW (Supporting Information). Together, these data suggest a basis for the fitness and motility defects of the OM.

**Fitness Costs Delay the Evolution of Resistance and Alter Evolutionary Trajectories.** WT populations in NIT SAGE plates (maximum [NIT] = 80  $\mu\text{g}/\text{mL}$ ; WT MIC: 8  $\mu\text{g}/\text{mL}$ ) evolved resistance to NIT in a predictable pattern (Figure S2A). All 16 replicates evolved in parallel stopped at  $\sim 30$  mm after 24 h, suggesting that the concentration of antibiotic was growth inhibiting at this point (Figure 2A,B). By day 2, all replicates broke through this and a subsequent barrier, fanning out in cones. By the end of day 4, all replicates reached the end of their lanes. Cells extracted from this point had an MIC against NIT of 64  $\mu\text{g}/\text{mL}$  (quantified from a randomly selected replicate, R3). Genome sequencing suggests that resistance to NIT evolved via mutations in the nitroreductase genes *nfsA* and *nfsB*, and *mprA*, repressor of the *marRAB* operon (Supporting Information). These genes have been commonly associated with nitrofurantoin resistance.<sup>34,35</sup> The purpose of the 29 other mutations in this strain is unclear. Many are involved in metabolism and may help compensate for the fitness cost of the resistance-conferring mutations. They may also be due to genetic drift as a number of them were in intergenic regions.

After a pilot run of OM in NIT SAGE ( $n = 4$ ) showed that the bacteria remained confined to within 10 mm of the inoculation site after 24 h (data not shown), we tested for collateral sensitivity of the OM toward NIT. We found the MIC of NIT against OM to be eight-fold lower (1  $\mu\text{g}/\text{mL}$ ) compared to WT. To the best of our knowledge, collateral sensitivity to nitrofurantoin in CHL-resistant cells has not been reported before. We then repeated evolutions with the OM ( $n = 16$ ), adjusting the NIT gradient to accommodate this increased sensitivity (maximum [NIT] = 10  $\mu\text{g}/\text{mL}$ ), as has been previously carried out to eliminate effects of collateral sensitivity on resistance evolution.<sup>20</sup> In contrast to the WT, movement of OM replicates through NIT SAGE plates showed large variation (Figure S2B). Cells were again confined to within  $\sim 10$  mm of the inoculation site after 24 h (Figure 2A,C), suggesting that the increased sensitivity to NIT was not the cause behind this impaired movement. The stationary

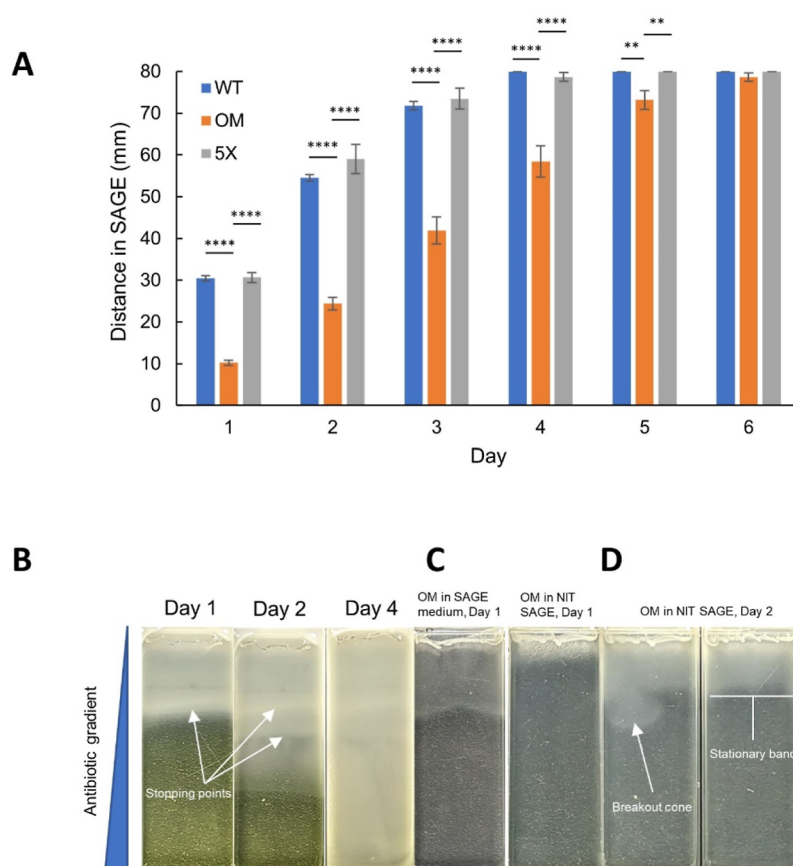


**Figure 2.** Tracking movement of bacterial populations in SAGE revealed resistance evolution impairments. (A) WT populations in NIT SAGE plates (maximum [NIT] = 80  $\mu\text{g}/\text{mL}$  for the WT, 10  $\mu\text{g}/\text{mL}$  for OM and 5X to accommodate hypersensitivity) evolve resistance faster than the OM. Alleviation of fitness deficits in the 5X population allows restoration of WT-like SAGE kinetics. (B) Stopping points of bacterial fronts indicate inhibitory antibiotic concentrations along the NIT gradient. Cells breaking free from these points indicate emergence of resistance mutation(s) that allow movement into higher antibiotic concentrations. All WT replicates reached the end of their lanes by the end of day 4. (C) Reduced growth and motility of the OM slow their movement speeds in SAGE but cannot explain the initial delay in distance moved in NIT SAGE plates. Left panel shows a representative lane where the OM moved  $\sim 30$  mm down a SAGE lane containing no antibiotic after 24 h. The right panel shows the OM confined to  $\sim 10$  mm after 24 h in a NIT SAGE lane (maximum [NIT] = 10  $\mu\text{g}/\text{mL}$ ). (D) Observing growth patterns in SAGE allows prediction of resistance emergence. On day 2 in NIT SAGE plates, only 5/16 replicates broke out from the initial stationary bands (left panel), indicating resistance emergence. The rest of the replicates remained as stationary bands (right panel), suggesting delayed resistance evolution. MIC measurements of cells from a breakout cone and stationary band confirmed these predictions (see the text).  $**p < 0.01$ ,  $***p < 0.0001$  from two-sample  $t$ -test assuming unequal variances. Error bars represent the SEM.  $N = 16$  for all SAGE evolutions.

phase cell density of the OM was  $\sim$ five-fold lower than the WT (Figure 1B). Since population size can affect evolution by altering mutation supply rates,<sup>36</sup> we also inoculated NIT SAGE plates separately with a five-fold concentrated inoculum of the OM ( $n = 4$ ). We observed no significant difference in distance moved, except on day 3, where the mean distance moved by the unstandardized OM (overnight culture) was higher than that by the standardized inoculum ( $p = 0.047$ ) (Table S1). Hence, we decided to conduct subsequent experiments with overnight cultures. We also noticed that although fitness deficits in OM impeded the strain's ability to move through soft agar, the movement in NIT SAGE plates at 24 h was  $\sim 1/3$  the growth in antibiotic-free soft agar. This is significantly slower than expected from changes in movement speed alone (Figure 2C).

The increased susceptibility of the OM populations may instead be due to their reduced growth rates. A recent study described how fast-growing cells avoid the intracellular accumulation of antibiotics like macrolides.<sup>37</sup> Although growth rates have not been directly linked to NIT susceptibility before,

it has been shown that cells that stay locked in a non-dividing state in lon mutants resistant to tetracyclines are known to exhibit increased sensitivity toward nitrofurantoin.<sup>38</sup> By counting the number of OM replicates that showed visible growth beyond the first stopping point (Figure 2D), we found that resistance emerged in only 5/16 replicates by the end of day 2. The link between position in the SAGE plate and resistance levels was verified by probing cells drawn from a randomly selected replicate from each position. The MIC of cells (R16) from stationary bands with no signs of "breakouts" was 1  $\mu\text{g}/\text{mL}$ , significantly less than that of cells extracted from breakout cones (R14, 8  $\mu\text{g}/\text{mL}$ ). By the end of day 6, all replicates generated mutants resistant to nitrofurantoin [MIC (R14): 8  $\mu\text{g}/\text{mL}$ ], with cells spreading throughout the lanes (Figure 2A). Of note, the MIC increase, although eight-folds higher than the base MIC of the OM (from 1 to 8  $\mu\text{g}/\text{mL}$ ), was equal to the base MIC of the WT.

Sequencing of the NIT-evolved OM (R14) did not reveal mutations in any of the genes commonly associated with NIT resistance (*nfsA*, *nfsB*, *ribE*, *oqxA*, *oqxB*, *mprA*, *oxyR*, *marA*, *rob*,

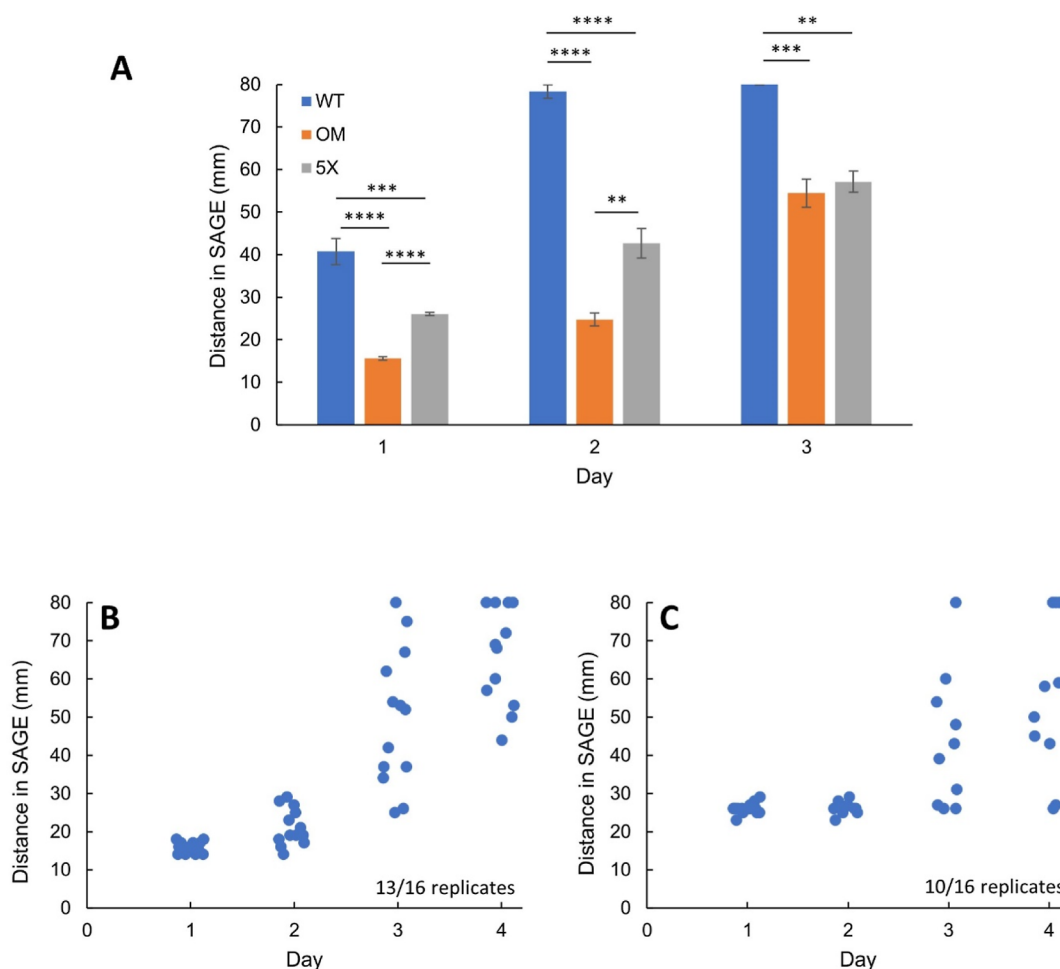


**Figure 3.** STR resistance is delayed in the fitness-impaired OM background. (A) WT replicates reached the end of STR SAGE plates (max [STR] = 160  $\mu\text{g}/\text{mL}$ ) by the end of day 2, whereas significant delays were observed for both the OM and the 5X populations. (B) 13/16 of the OM replicates remained at  $\leq 29$  mm in STR SAGE lanes at the end of day 2, indicating delayed resistance evolution. (C) Delay in STR resistance could not be alleviated via fitness improvements as 10/16 replicates remained completely stationary at the end of day 2 after hitting their inhibitory concentration step on day 1. Resistance-level predictions were confirmed by MIC measurements from cells sampled from random replicates (see the text). \*\* $p < 0.01$ , \*\*\* $p < 0.001$ , \*\*\*\* $p < 0.0001$  from two-sample  $t$ -test assuming unequal variances. Error bars represent the SEM.  $N = 16$  for all SAGE evolutions.

*soxS*, *sdsN137*)<sup>34,35</sup> (Supporting Information). It showed nine non-synonymous mutations compared to the OM, most of which were in genes related to metabolism. Interestingly, it also contained a second mutation in *lolA*. The OM strain natively harbored a mutation in the periplasmic chaperone protein LolA, which is essential for lipoprotein trafficking through the periplasm to the outer membrane and membrane integrity.<sup>39</sup> The outer membrane presents a barrier to a number of antibiotics including nitrofurantoin,<sup>39,40</sup> and it is hence possible that the mutation in LolA increases cellular access to nitrofurantoin, producing the observed collateral sensitivity. LolA mutants are also known to be severely growth-challenged.<sup>41</sup> The second mutation in the NIT-evolved OM could then compensate for the increased membrane permeability and growth defect, alleviating the collateral sensitivity toward NIT and allowing these mutants to traverse the SAGE plates without acquiring NIT-resistance mutations. This trajectory has the dual advantage of improving fitness and bypassing collateral sensitivity toward the antibiotic they were put up against. A similar phenomenon was observed in a previous study,<sup>21</sup> where during a treatment switch from gentamicin to carbenicillin, a drug-pair that shows reciprocal

collateral sensitivity, resensitization to gentamicin may have been favored over multidrug resistance due to trajectories that mitigate both fitness costs and collateral sensitivity. Although we cannot discount the possibility of downregulation of the classical genes involved in NIT-resistance, no mutations were found in any known transcriptional regulators.

**Evolution against Streptomycin.** To test if the delay in resistance evolution is limited to nitrofurantoin, we compared resistance evolution to an unrelated antibiotic, the aminoglycoside streptomycin (STR). In WT populations subjected to STR SAGE (maximum [STR] = 160  $\mu\text{g}/\text{mL}$ ; WT MIC: 16  $\mu\text{g}/\text{mL}$ ), resistance evolved via a clear, repeatable trajectory wherein cells stopped at  $\sim 40$  mm (Figures 3A, S2C) after 24 h, with mutants breaking free from this stopping point within 48 h. The STR MIC of cells at the first stopping point showed a two-fold increase (MICs (R14, R15): 32  $\mu\text{g}/\text{mL}$ ) while by the end of day 2, MICs rose to  $>1024$   $\mu\text{g}/\text{mL}$ , indicating the emergence of ribosomal mutations (MICs from R9–R16).<sup>42</sup> The two-fold increase in STR resistance that appeared on day 1 reverted to WT levels after cells were subcultured in antibiotic-free medium. This may either indicate selection for a heteroresistant population or the emergence of unstable

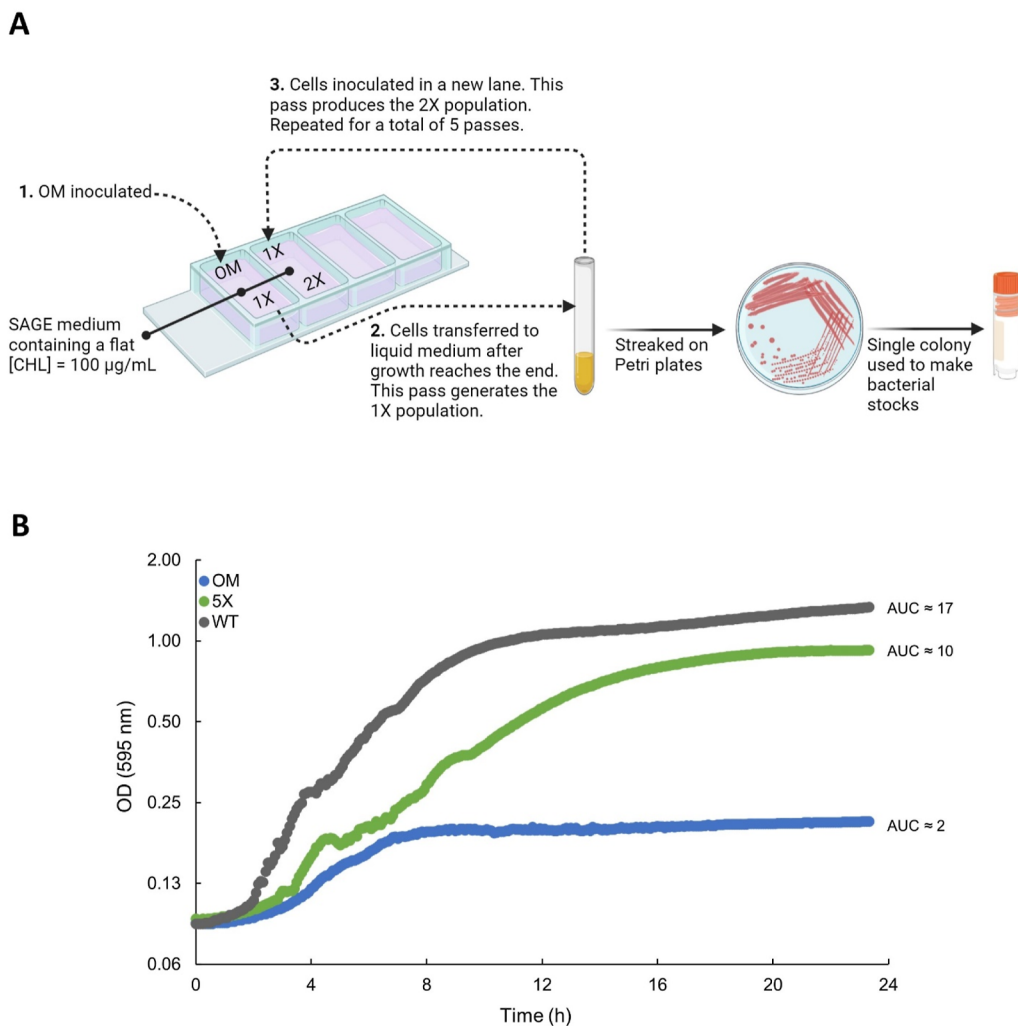


**Figure 4.** Passaging cells through “flat” SAGE lanes improves fitness of the OM. (A) OM cells are inoculated in SAGE lanes containing a constant [CHL] = 100 µg/mL. Fitter cells move out to the end of the lanes first, which are then extracted and cultured. These cells are denoted 1X. The 1X is inoculated back in a new, identical flat lane to generate 2X. This cycle was repeated until the generation of 5X. Cells were passed on Petri plates, and bacterial stocks were prepared after each cycle. (B) 5X shows significant improvement in fitness as shown by the AUC.

resistance mutations upon which ribosomal mutations arise.<sup>43,44</sup>

We evolved the OM in SAGE plates using the same parameters used for the WT since the MIC of STR against both the OM and WT populations were equal. The OM again travelled ~half the distance covered by the WT in 24 h in STR SAGE plates (Figure 3A).

Increased susceptibility to antibiotics that bind irreversibly to ribosomes like STR in growth-impaired bacterial populations has been reported before.<sup>45</sup> This repeated slow movement in antibiotic gradients may also indicate the importance of bacterial fitness in their intrinsic ability to resist antibiotics. The majority of the replicates (13/16) stopped at  $\leq 29$  mm after 48 h (Figure 3B). Out of the two replicates sampled to quantify STR MIC against cells from this point (R3 and R8), R8 showed an MIC of 128 µg/mL (with R3 an MIC of 32 µg/mL). This suggested that resistance to STR in the OM populations may evolve via alternate trajectories and encouraged us to expand the sample size. Since we did not sample more than two replicates from day 2, and attempting to extract mutants that arose on day 2 at a later time point could include higher-order mutants that could compromise the MIC

results, we instead extracted end-point mutants from a total of eight replicates (R1, R5, R7, R8, R9, R12, R13, and R16) and compared them with the eight WT end-point mutants. While all WT mutants showed an MIC > 1024 µg/mL, two out of the eight OM replicates (R9, R12) showed an MIC of 512 µg/mL, further suggesting the adoption of alternate evolutionary paths to resistance by the OM. Sequencing an STR-evolved WT replicate (R5) showed an expected K43R mutation in *rpsL*, the gene that codes for the S12 protein of the 30S subunit of the ribosome, the target for streptomycin.<sup>46</sup> The replicate also evolved 15 additional mutations on genes broadly involved in metabolism, membrane transport, and integrity (Supporting Information). Mutations in *letB* (D40G) and *rutG* (synonymous, A46A), which are involved in membrane integrity, may also contribute to mild STR resistance since membrane stability and voltage dysregulation are implicated in the bactericidal effects of STR.<sup>40,47,48</sup> Although synonymous (A48A), mutations in the outer membrane lipoprotein YaiW have been associated with mild STR resistance before by reducing membrane permeability.<sup>49</sup> We also sequenced three replicates of the STR-evolved OM (R7, MIC: >1024 µg/mL; R9, R12, MIC: 512 µg/mL) to identify possible differences in

their genome that could explain the differences in MIC. All the three STR-evolved OM replicates contained an *rpsL* mutation (K88R, K88R, and K43R, respectively), along with mutations in *yqfA*, *bcsB*, and *pfID* in the same position in all three replicates (I127V, A390A, and P658S, respectively). Mutations in these three genes were not found in the WT, or in any other strain sequenced in this study. YqfA is involved in the maintenance of optimal membrane energetics and may hence play a role in STR resistance.<sup>47</sup> *BcsB*, part of the operon *bcsQ*, codes for a protein with a predicted function in cellulose biosynthesis, but *E. coli* MG1655 contains a stop codon after the first five amino acids of the operon.<sup>50,51</sup> Its repeated appearance in all three replicates of the STR-adapted OM may indicate an involvement in either STR resistance or in the mitigation of fitness costs, but literature contains no evidence of these. PfiD is a putative pyruvate formate-lyase and may be an easily accessible compensatory mutation to mitigate fitness deficits via enhancing anaerobic sugar metabolism.<sup>52,53</sup> All three replicates also contained a mutation in tRNA-gln (identical C → T mutation in glnX in R7 and R12, and a C→T mutation in glnV in R9), which has been reported in STR-resistant *E. coli* before, and may confer a fitness benefit.<sup>49</sup> Additionally, R9 harbored another ribosomal mutation in the 30S ribosomal subunit protein S7 encoded by *rpsG*. S7 is a translational repressor regulating the synthesis of other gene products including S12 (*rpsL*) and has not been directly linked to STR resistance in *E. coli*. Multiple mutational screens of *rpsG* in other species like *Mycobacterium smegmatis* and *Borrelia burgdorferi* found no evidence of involvement in STR resistance.<sup>54,55</sup> The rest of the non-overlapping mutations among these three replicates and the STR-evolved WT are mostly in genes involved in metabolism. Taken together, these results suggest that mutational paths to resistance to streptomycin in fitness-impaired *E. coli* diverges from that taken by WT, and although all the OM-replicates evolved an *rpsL* mutation, MIC measurements suggest that interactions between the non-overlapping mutations may be reducing the resistance level below what is expected of *rpsL* mutants.<sup>56</sup>

**Improving Fitness of Chloramphenicol-Resistant Cells Restores Resistance Potential to Nitrofurantoin but Not Streptomycin.** To test if alleviating the fitness deficits of the resistant cells improves NIT resistance evolution during SAGE, we serially passaged the OM a total of five times through “flat” SAGE medium containing a constant 100  $\mu\text{g}/\text{mL}$  (MIC: 256  $\mu\text{g}/\text{mL}$ ) of CHL (Figure 4A). Cells that reached the end of the lanes were extracted after each pass (denoted 1X–5X). Growing in a constant, permissible concentration of antibiotic, nutrient scarcity and overcrowding becomes the primary driver of evolution, driving selection for fitter cells that can quickly move out to access nutrients and reach the end of the lanes first.<sup>57</sup> In vitro, this increase in fitness generally arises from compensatory mutations that mitigate fitness costs.<sup>30</sup> Growth curves of 1X–5X showed significant improvements in fitness with AUCs  $\sim$ 5-times above the OM but without much difference within the series (Figure 4B) (Figure S1). The movement speed of 5X through soft agar was also significantly improved, with the strain requiring only 8 h to traverse half the plate compared to 24 h by the OM (Movie S1). However, 1X–5X all maintained their CS toward NIT. Genome sequencing of 5X revealed 17 mutations in genes mostly involved in metabolism (Supporting Information). Importantly, it removed the loss-of-function mutation (introduction of a stop codon) in the flagellar protein FlgG

that the OM previously acquired (TAG → TGG). This strain also harbored an additional mutation in *rpoD*, which codes for an RNA polymerase sigma factor essential for exponential growth, and may be compensating for an *rpoD* mutation in the OM. A mutation was also identified in the methyl-accepting chemotaxis protein Tsr. These mutations may help explain the improved fitness of the 5X.

We then repeated the NIT SAGE evolutions with 5X ( $n = 16$ ). The evolutionary kinetics of the 5X closely mirrored that of the WT (Figure 2A), implicating the fitness cost of CHL resistance to be the principal cause behind the slower adaptation to nitrofurantoin. The NIT MIC of cells extracted from one of these plates was 32  $\mu\text{g}/\text{mL}$  (R8). Sequencing these cells revealed mutations in *nfsA* and *nfsB*, albeit in positions distinct from that in the WT (Supporting Information). Unexpectedly, the NIT-evolved 5X also showed a large 6279 bp deletion which includes the entire *marRAB* operon, and the genes encoding YdeA (L-arabinose exporter of the major facilitator superfamily of transporters),<sup>58</sup> MarC (DNA-binding transcriptional dual regulator SoxR),<sup>59</sup> EamA (exporter of metabolites of the cysteine pathway),<sup>60</sup> YdeE (Drug/H<sup>+</sup> antiporter-1 within the major facilitator superfamily of transporters),<sup>61</sup> MgtS (involved in intracellular Mg<sup>2+</sup> accumulation),<sup>62</sup> mgtT (involved in intracellular Mg<sup>2+</sup> accumulation),<sup>63</sup> MgrR (negative regulator of SoxS),<sup>64</sup> and DgcZ (a diguanylate cyclase that regulates motility and biofilm formation).<sup>65</sup> Mutations in nitroreductase enzymes have been previously linked to growth defects,<sup>66</sup> and it is possible that nitroreductase mutations are incompatible with overexpression of efflux pumps, i.e., the combination may impose debilitating fitness defects. The absence of nitroreductase mutations in the NIT-evolved OM also supports this idea. Removal of the *marRAB* operon and the other efflux pumps would then allow curbing the energy costs of the efflux systems, allowing access to nitroreductase mutations. To test this hypothesis, we compared the CHL MIC and growth curves of the NIT-evolved OM and 5X. CHL MIC of the NIT-evolved 5X showed a reduction below the OM level, while the NIT-evolved OM maintained the same resistance level. This reduction in MIC was less than two-fold, however, as the NIT-evolved 5X exhibited faint growth in the well containing 128  $\mu\text{g}/\text{mL}$  of CHL, as opposed to saturated growth at the same drug concentration with the NIT-evolved OM. The NIT-evolved 5X also showed a moderate increase in AUC ( $\approx$ 12) when compared to the NIT-evolved OM ( $\approx$ 9.5) (Figure S3). Much like the NIT-evolved WT, the other mutations in the NIT-evolved 5X were mostly in genes involved in metabolism and membrane transport, but in genes distinct from that in the WT. We found no overlapping mutations between the NIT-evolved OM and the NIT-evolved 5X.

In STR SAGE plates, the improved fitness of 5X allowed them to move  $\sim$ 1.5 times the distance moved by the OM in 24 h. However, 10/16 replicates remained completely stationary at this point for an additional 24 h before generating mutants (Figure 3C). The STR MIC against cells past this point was  $>1024 \mu\text{g}/\text{mL}$  (MICs quantified from R2, R3, R9, and R13). By day 3, there was no significant difference between the mean distance moved by the OM and 5X (Figure 3A). Sequencing of a STR-evolved 5X strain (R3) showed a K88R mutation in *rpsL*, along with 16 other non-synonymous mutations (Supporting Information). Outside the *rpsL* mutations, comparing the STR-evolved 5X with the STR-evolved OMs and the STR-evolved WT showed no overlapping mutations

except for the ones in genes that code for YfaL (a putative adhesin)<sup>67</sup> and RecD (a exodeoxyribonuclease V subunit),<sup>68</sup> which were shared between 5X R3 and OM R9 (in distinct positions), and in the curcumin reductase CurA between the 5X and the WT (in distinct positions, with the mutation in the WT being synonymous). Overall, while fitness-enhancement improved the movement speeds of bacterial cells in STR gradients, it could not restore WT adaptation rates to STR. Comparison of sequencing data of the STR-evolved WT, OM and 5X end-point mutants revealed mutations in different sets of genes (except for the resistance-conferring *rpsL* mutations), mostly coding for proteins essential in metabolism. Because the 5X still lagged behind the WT in terms of fitness (Figure 4B), this could either suggest a certain fitness threshold below which STR resistance is delayed or that the evolutionary paths to resistance available to a fitness-impaired background leads to slower adaptation.

**Impaired Resistance Evolution is Not Linked to Chloramphenicol Resistance.** To determine if the reduction in secondary adaptation rates were dependent on the primary antibiotic (i.e., CHL), we generated a CFZ-resistant mutant of *E. coli* K-12 substrain BW25113 (CFZR) (MIC > 512  $\mu\text{g}/\text{mL}$ ). This strain exhibited lower fitness compared to the WT *E. coli* BW25113 (WTB), though it was not as fitness impaired as OM (Figure S4A), able to traverse an entire antibiotic-free plate in 24 h (data not shown). When subject to a NIT challenge (maximum [NIT] = 80  $\mu\text{g}/\text{mL}$ ; WTB MIC: 8  $\mu\text{g}/\text{mL}$ ;  $n = 8$ ), CFZR evolved significantly slower than WTB (Figure S4B). Similar to the OM in NIT SAGE plates (Figure 2D), CFZR did not show signs of breakouts in any replicate lanes on day 2, while all WTB replicates broke free from their first stopping points. This suggests that the reduced rate of adaptation to NIT is independent of the CHL-resistance phenotype and/or the genetic background. This also shows that the magnitude of fitness deficit need not be as great as the difference between the OM and the WT for adaptation to be significantly impaired.

In contrast, a STR-resistant *E. coli* with no detectable fitness deficit (Figure S1, Movie S1) showed no delay in NIT resistance evolution (data not shown). We routinely recovered NIT-resistant cells from SAGE plates containing max [NIT] of 80  $\mu\text{g}/\text{mL}$  by passing them on standard selective agar plates containing 32  $\mu\text{g}/\text{mL}$  of NIT (4X MIC). While we were able to recover all replicates of the WTB on selective agar plates, we were only able to obtain three out of eight replicates of the CFZR, suggesting that the majority of the CFZR replicates, despite evolving under the same regime as WTB, developed lower levels of resistance.

## DISCUSSION

Sequential antibiotic therapies that involve changing the antibiotic applied after a duration of treatment have been proposed as a strategy to reduce resistance evolution and improve bacterial clearance.<sup>17</sup> Our study shows that fitness defects due to evolution of resistance to an initial antibiotic can impede the ability of bacteria to adapt to subsequent antibiotics. While growth and fitness measurements can indicate fitness deficits that may lead to reduced adaptation rates, the utility of these effects is contingent on the repeatability of evolution and the frequency with which escape mutants emerge.<sup>18</sup> Large numbers of parallel *in vitro* evolution experiments are required to account for the stochasticity of evolution. We previously reported the ability of the SAGE

system to generate resistance to antibiotics from every major class-effective against Gram-negative bacteria.<sup>22</sup> Here, we leverage its ability to run parallel evolutions in the laboratory to show that fitness deficits associated with resistance to CHL repeatedly impede evolution to secondary antibiotics (Figures 2 and 3). Because the OM showed a multidrug resistance phenotype, possibly due to hyperactive efflux, we investigated adaptation to streptomycin and nitrofurantoin; two drugs that are not efficient efflux targets.<sup>29</sup> Both drugs also exhibit predictable and highly repeatable evolution kinetics in SAGE.

We found that the rate of distance moved by bacteria in SAGE plates is a robust indicator of the adaptation rates to antibiotics since it integrates the rate at which resistance-conferring mutations appear with bacterial growth rates and motility. By running 16 replicates in parallel and tracking mutants by their distance moved in SAGE and their growth patterns (Figures 2 and 3), we found that escape mutants that bypassed this delay arose at low frequencies (5/16 for OM evolving to NIT and 3/16 for OM evolving to STR). MIC values from cells extracted from different positions of SAGE plates aligned well with the expected phenotype.

The delayed adaptation to antibiotics could not be alleviated by equalizing the number of cells added to the SAGE plates (Table S1). This may suggest that the increase in mutation supply rate that comes with a larger population<sup>36</sup> may not be enough to compensate for the slow cell turnover rate<sup>69</sup> and the adoption of suboptimal evolutionary trajectories due to epistatic interactions<sup>56</sup> that both reduce antibiotic susceptibility and improve fitness.

Probing cells from different points of growth from SAGE plates can provide insights into evolutionary trajectories. By measuring the MIC of antibiotics against cells from stationary bands collected 24 h into the STR evolution studies, we identified unstable resistant mutants upon which higher-order, stable mutants arose. This is a phenomenon which, to the best of our knowledge, has not been reported for streptomycin before. We also found that two out of the eight STR-evolved OM replicates showed higher susceptibility to STR (MIC: 512  $\mu\text{g}/\text{mL}$ ) than STR-evolved WT replicates (MIC > 1024  $\mu\text{g}/\text{mL}$  for all eight replicates tested). While the MIC values for these replicates are clearly above the clinical breakpoint of STR, it is interesting to note that compensatory mutations that arise to mitigate fitness defects can negatively affect the resistance levels conferred by resistance-conferring mutations.

Generation of fitter mutants through compensatory mutations generally requires continuous subculturing, often for several months.<sup>70,71</sup> A total of five serial passages through soft agar over approximately 2 weeks generated CHL-resistant mutants (SX) markedly fitter than the OM (Figure 4), with AUC comparable to the WT (Figure 4B). When comparing OM and 5X populations adapting to NIT in SAGE plates with identical NIT gradients (maximum [NIT] = 10  $\mu\text{g}/\text{mL}$ ), resistance in the OM replicates was significantly delayed while the 5X leveled their rates to the WT (Figure 2A). SX also evolved a higher MIC than the OM, which surpassed the maximum concentration of NIT encountered in the plates by about three-fold (OM, R14: 8  $\mu\text{g}/\text{mL}$ ; SX, R8: 32  $\mu\text{g}/\text{mL}$ ). This “overshoot” in resistance has been reported before and has important consequences since bacteria encountering sub-lethal concentrations of antibiotics can evolve resistance beyond clinical breakpoints.<sup>20</sup> Sequencing revealed that the OM did not acquire mutations in any genes implicated in NIT resistance, while the SX evolved resistance via mutations in the

nitroreductase enzymes classically known to confer NIT resistance. Together, this shows that resistance mechanisms that incur large fitness costs may delay the evolution of resistance and favour, at least when subjected to lower concentrations of antibiotics, the adoption of evolutionary paths that mitigate existing fitness costs over resistance evolution. Contrary to what was observed for NIT, the fitter 5X populations could not restore their STR adaptation potential to WT levels, with resistance being delayed by a day in the majority of the replicates (10/16 replicates) (Figure 3C). Sequencing revealed *rpsL* mutation in the 5X replicate, with the rest of the mutational profile mostly distinct from that of the STR-adapted WT and OM (Supporting Information). The underlying reason behind this slowdown in evolution to STR could not be determined, but the inability to alleviate this slowdown even after multiple passes through SAGE medium suggests that this may be a stable phenotype. Identification of fitness deficits that are stable at the face of fitness-compensation is a major step toward translation of evolutionary trade-offs into effective therapy.<sup>72</sup>

The design of sequential antibiotic therapy is not trivial. The primary antibiotic must be selected such that the evolutionary pathways impose deficits that impede subsequent adaptation. A STR-mutant barely exhibits any fitness defects (Figure S1), and would not be expected to deviate in evolutionary kinetics from that of the WT (we tested the ability of STR-mutants to generate resistance to NIT in 4 replicates, and did not observe any significant difference from the WT; data not shown). Streptomycin is also antagonized by the bacteriostatic CHL when applied in combination.<sup>73</sup> Sequential application of antagonistic drugs, in the correct direction, may be a practical option over combination approaches to slow resistance evolution.

In sequential antibiotic regimens where an antibiotic is applied for a short period of time, the antibiotic may not be able to completely eradicate a population that remains at WT resistance levels.<sup>74</sup> Upon cessation of therapy, the WT population may then possess a selective advantage over the antibiotic-resistant populations that are often growth impaired. A recent publication also showed how fast-growing bacterial populations can counteract antibiotic susceptibility to dominate bacterial communities independent of specific antibiotic mechanisms.<sup>75</sup> Since not all antibiotic resistance mechanisms incur fitness costs,<sup>76</sup> resistance mechanisms that do are important to identify.

\*\*The mutations conferring resistance to CHL in the bacterial strain used in this study are primarily linked to upregulation of non-specific efflux pumps, not to alterations in how CHL binds to its target. Since resistance to a wide range of antibiotics is often conferred via mutations in efflux pumps,<sup>6,64</sup> we expect the rate of resistance evolution to decrease when bacteria evolve resistance to antibiotics via upregulation of these systems and potentially via other adaptations with significant fitness penalties. This effect may also be independent of the genetic background. To support this notion, we showed that the OM is resistant to a variety of antibiotics (Table 1), and a cephalosporin-resistant mutant of *E. coli* K-12 substrain BW25113 that exhibited significant fitness defects also exhibited slower adaptation to NIT (Figure S4). Furthermore, the fitness-impaired CFZR frequently evolved lower resistance levels than the WT strain (S/8 replicates).

Overall, our findings suggest that the fitness costs associated with antibiotic resistance may be exploited to slow down resistance evolution, and the SAGE system can be utilized to identify evolutionarily stable impairments at high-throughput. We hope that studies like this can guide optimal drug switches to develop sequential antibiotic therapies that are less prone to resistance evolution.

## ■ MATERIALS AND METHODS

**Bacterial Strain and Growth Conditions.** *E. coli* K-12 substrain MG1655 (WT) and all subsequent resistant mutants were grown in Mueller Hinton (MH) media at 37 °C. Growth media was supplemented with appropriate antibiotics when growing mutants or extracting mutants from SAGE plates.

**SAGE Evolutions.** SAGE plates were prepared as described previously.<sup>22</sup> Briefly, 6 mL of MH media + 0.25% agar (MHA) supplemented with appropriate antibiotic was poured into each lane of four-well dishes (Thermo Fisher Scientific, Cat. no. 167063) propped up on one side using p1000 pipette tips. Antibiotic concentrations suitable for evolutions were determined via prior MIC testing. The resulting wedge-shaped media were left to set for ~20 min before removing the pipette tips and pouring 8 mL of antibiotic-free MHA. The plates were left at room temperature overnight to allow diffusion to set up the antibiotic gradient. 50  $\mu$ L of overnight bacterial culture was inoculated in a line 1–2 mm below the agar surface in each lane, overlaid with ~2.5 mL of mineral oil to reduce drying by evaporation, and incubated at 37 °C. Plates were checked every 24 h to measure maximum distance moved by the bacterial fronts. Resistant mutants were extracted by cutting out ~5  $\times$  5 mm sections from the end of the plates and dispersing in MH broth (MHB). For the generation of the OM, these mutants were inoculated back into a second CHL-gradient (Figure 1A).

**Growth Measurements.** Absorbance readings at 595 nm of 1/200 dilutions of overnight cultures were recorded using a plate reader (Tecan Sunrise). To reduce fogging of the plates which interferes with absorbance readings, plate lids were made hydrophilic by pouring in 3 mL of 0.05% Triton X-100 in 20% ethanol and swirling to ensure coverage. After 30 s, excess solution was discarded, and lids were air dried.<sup>77</sup> Growth curves were fitted to a logistic equation, and AUCs were calculated using the R package *growthcurver*.<sup>78</sup>

**Fitness Improvements via Flat-Concentration SAGE Plates.** ~13 mL of MHA was poured in a lane of four-well dishes containing 100  $\mu$ g/mL of CHL. Once set, 50  $\mu$ L of overnight bacterial culture, was inoculated as described before. After growth reached the end of lanes (16–20 h of incubation for 1X–5X, ~48 h for OM), cells were extracted by cutting out ~5  $\times$  5 mm sections from the end of plates and dispersing in 5 mL of MHB supplemented with 100  $\mu$ g/mL of CHL. Extracted cells were incubated and used as the inoculum for the next flat lane, up to a total of five passages to generate the 5X strain (Figure 4A).

**MIC Assays.** MICs were determined as recommended by CLSI.<sup>79</sup> Briefly, 10 point dilutions of antibiotics were made in MHB and inoculated with a 1/200 dilution of 0.5 McFarland standardized inoculum. Plates were incubated overnight, and MICs were recorded as the minimum concentration of antibiotic that resulted in no visible growth.

**Whole Genome Sequencing.** Sequencing and variant calling were performed by Seqcenter (USA). Sequencing was performed on an Illumina NextSeq 2000, and demultiplexing,

quality control, and adapter trimming was performed with bcl-convert (v3.9.3). Variant calling was carried out using Breseq under default settings.<sup>80</sup> NCBI reference sequence NC\_000913.3 for *E. coli* K-12 substrain MG1655 was used for variant calling. Sequencing data have been deposited in the NCBI BioProject database with accession number PRJNA986536. Sequencing quality information is reported in the [Supporting Information](#)

## ■ ASSOCIATED CONTENT

### SI Supporting Information

The Supporting Information is available free of charge at <https://pubs.acs.org/doi/10.1021/acsinfecdis.3c00156>.

Additional growth curves, kinetics of nitrofurantoin evolution, and inoculum effect (PDF)

Variant calling data, depths/allele frequencies of each call, and genome sequencing quality information (XLSX)

Bacteria motility in antibiotic-free SAGE medium; inoculated with WT *E. coli* MG1655 and STR-resistant *E. coli* MG1655, OM, and SX (MP4)

## ■ AUTHOR INFORMATION

### Corresponding Author

Brandon L. Findlay – Department of Biology and Department of Chemistry and Biochemistry, Concordia University, Montréal, Québec H4B 1R6, Canada; [orcid.org/0000-0001-7083-2513](https://orcid.org/0000-0001-7083-2513); Email: [brandon.findlay@concordia.ca](mailto:brandon.findlay@concordia.ca)

### Author

Farhan R. Chowdhury – Department of Biology, Concordia University, Montréal, Québec H4B 1R6, Canada

Complete contact information is available at: <https://pubs.acs.org/doi/10.1021/acsinfecdis.3c00156>

### Notes

The authors declare no competing financial interest.

## ■ ACKNOWLEDGMENTS

We thank Prerna Singh (PhD student, Findlay Lab) for developing and supplying the CFZ-resistant strain. We are grateful to Dr. Lisa Freeman for helpful discussions. This work was supported by the fonds de recherche du Québec—Santé (FRQS) (269182). Figures <sup>1</sup>A and <sup>4</sup>A, and the TOCs were created with Biorender.com.

## ■ REFERENCES

(1) Murray, C. J.; Ikuta, K. S.; Sharara, F.; Swetschinski, L.; Robles Aguilar, G.; Gray, A.; Han, C.; Bisignano, C.; Rao, P.; Wool, E.; Johnson, S. C.; Browne, A. J.; Chipeta, M. G.; Fell, F.; Hackett, S.; Haines-Woodhouse, G.; Kashef Hamadani, B. H.; Kumaran, E. A. P.; McManigal, B.; Achalalpong, S.; Agarwal, R.; Akech, S.; Albertson, S.; Amuasi, J.; Andrews, J.; Aravkin, A.; Ashley, E.; Babin, F. X.; Bailey, F.; Baker, S.; Basnyat, B.; Bekker, A.; Bender, R.; Berkley, J. A.; Bethou, A.; Bielicki, J.; Boonkasidecha, S.; Bukosia, J.; Carvalheiro, C.; Castañeda-Orjuela, C.; Chansamouth, V.; Chaurasia, S.; Chiurchiù, S.; Chowdhury, F.; Clotire Donatien, R.; Cook, A. J.; Cooper, B.; Cressey, T. R.; Criollo-Mora, E.; Cunningham, M.; Darboe, S.; Day, N. P. J.; De Luca, M.; Dokova, K.; Dramowski, A.; Dunachie, S. J.; Duong Bich, T.; Eckmanns, T.; Eibach, D.; Emami, A.; Feasey, N.; Fisher-Pearson, N.; Forrest, K.; Garcia, C.; Garrett, D.; Gastmeier, P.; Giref, A. Z.; Greer, R. C.; Gupta, V.; Haller, S.; Haselbeck, A.; Hay, S. I.; Holm, M.; Hopkins, S.; Hsia, Y.; Iregbu, K. C.; Jacobs, J.; Jarovsky,

D.; Javanmardi, F.; Jenney, A. W. J.; Khorana, M.; Khusuwan, S.; Kisson, N.; Kobeissi, E.; Kostyanov, T.; Krapp, F.; Krumkamp, R.; Kumar, A.; Kyu, H. H.; Lim, C.; Lim, K.; Limmathurotsakul, D.; Loftus, M. J.; Lunn, M.; Ma, J.; Manoharan, A.; Marks, F.; May, J.; Mayxay, M.; Mturi, N.; Munera-Huertas, T.; Musicha, P.; Musila, L. A.; Mussi-Pinhata, M. M.; Naidu, R. N.; Nakamura, T.; Nanavati, R.; Nangia, S.; Newton, P.; Ngoun, C.; Novotney, A.; Nwakanma, D.; Obiero, C. W.; Ochoa, T. J.; Olivas-Martinez, A.; Oliario, P.; Ooko, E.; Ortiz-Brizuela, E.; Ounchanum, P.; Pak, G. D.; Paredes, J. L.; Peleg, A. Y.; Perrone, C.; Phe, T.; Phommason, K.; Plakkal, N.; Ponce-de-Leon, A.; Raad, M.; Ramdin, T.; Rattanavong, S.; Riddell, A.; Roberts, T.; Robotham, J. V.; Roca, A.; Rosenthal, V. D.; Rudd, K. E.; Russell, N.; Sader, H. S.; Saengchan, W.; Schnall, J.; et al. Global Burden of Bacterial Antimicrobial Resistance in 2019: A Systematic Analysis. *Lancet* **2022**, *399*, 629–655.

(2) Jacobs, A. U. N. Issues Urgent Warning on the Growing Peril of Drug-Resistant Infections. *The New York Times*. April 29, 2019. <https://www.nytimes.com/2019/04/29/health/un-drug-resistance-antibiotics.html> (accessed Aug 28, 2022).

(3) Dadgostar, P. Antimicrobial Resistance: Implications and Costs. *Infect. Drug Resist.* **2019**, *12*, 3903–3910.

(4) Van Boeckel, T. P.; Pires, J.; Silvester, R.; Zhao, C.; Song, J.; Criscuolo, N. G.; Gilbert, M.; Bonhoeffer, S.; Laxminarayan, R. Global Trends in Antimicrobial Resistance in Animals in Low- and Middle-Income Countries. *Science* **2019**, *365*, No. eaaw1944.

(5) Rolfe, R.; Kwobah, C.; Muro, F.; Ruwanpathirana, A.; Lyamuya, F.; Bodinayake, C.; Nagahawatte, A.; Piyasiri, B.; Sheng, T.; Bollinger, J.; Zhang, C.; Ostbye, T.; Ali, S.; Drew, R.; Kussin, P.; Anderson, D. J.; Woods, C. W.; Watt, M. H.; Mmbaga, B. T.; Tillekeratne, L. G. Barriers to Implementing Antimicrobial Stewardship Programs in Three Low- and Middle-Income Country Tertiary Care Settings: Findings from a Multi-Site Qualitative Study. *Antimicrob. Resist. Infect. Control.* **2021**, *10*, 60.

(6) Jacobs, A. W. H. O. Warns That Pipeline for New Antibiotics Is Running Dry. *The New York Times*. January 17, 2020. <https://www.nytimes.com/2020/01/17/health/antibiotics-resistance-new-drugs.html> (accessed Aug 28, 2022).

(7) Merker, M.; Tueffers, L.; Vallier, M.; Groth, E. E.; Sonnenkalb, L.; Unterweger, D.; Baines, J. F.; Niemann, S.; Schulenburg, H. Evolutionary Approaches to Combat Antibiotic Resistance: Opportunities and Challenges for Precision Medicine. *Front. Immunol.* **2020**, *11*, 11.

(8) Dawes, E. A. Growth and Survival of Bacteria. In *Bacteria in Nature: Volume 3: Structure, Physiology, and Genetic Adaptability*; Poindexter, J. S., Leadbetter, E. R., Eds.; *Bacteria in Nature*; Springer US: Boston, MA, 1989; pp 67–187. DOI: [DOI: 10.1007/978-1-4613-0803-4\\_2](https://doi.org/10.1007/978-1-4613-0803-4_2).

(9) Palma, V.; Gutiérrez, M. S.; Vargas, O.; Parthasarathy, R.; Navarrete, P. Methods to Evaluate Bacterial Motility and Its Role in Bacterial–Host Interactions. *Microorganisms* **2022**, *10*, 563.

(10) Geisel, N.; Vilar, J. M. G.; Rubi, J. M. Optimal Resting-Growth Strategies of Microbial Populations in Fluctuating Environments. *PLoS One* **2011**, *6*, No. e18622.

(11) Hepatology, T. L. G. The Problem of Antimicrobial Resistance in Chronic Liver Disease. *Lancet Gastroenterol. Hepatol.* **2022**, *7*, 495.

(12) Pailhoriès, H.; Herrmann, J.-L.; Velo-Suarez, L.; Lamoureux, C.; Beauruelle, C.; Burgel, P.-R.; Héry-Arnaud, G. Antibiotic Resistance in Chronic Respiratory Diseases: From Susceptibility Testing to the Resistome. *Eur. Respir. Rev.* **2022**, *31*, 210259.

(13) Nelson, C. P.; Hoberman, A.; Shaikh, N.; Keren, R.; Mathews, R.; Greenfield, S. P.; Mattoo, T. K.; Gotman, N.; Ivanova, A.; Moxey-Mims, M.; Carpenter, M. A.; Chesney, R. W. Antimicrobial Resistance and Urinary Tract Infection Recurrence. *Pediatrics* **2016**, *137*, No. e20152490.

(14) López-Causapé, C.; Rojo-Molinero, E.; Macià, M. D.; Oliver, A. The Problems of Antibiotic Resistance in Cystic Fibrosis and Solutions. *Expert Rev. Respir. Med.* **2015**, *9*, 73–88.

(15) Nichol, D.; Jeavons, P.; Fletcher, A. G.; Bonomo, R. A.; Maini, P. K.; Paul, J. L.; Gatenby, R. A.; Anderson, A. R. A.; Scott, J. G.

Steering Evolution with Sequential Therapy to Prevent the Emergence of Bacterial Antibiotic Resistance. *PLoS Comput. Biol.* **2015**, *11*, No. e1004493.

(16) Imamovic, L.; Sommer, M. O. A. Use of Collateral Sensitivity Networks to Design Drug Cycling Protocols That Avoid Resistance Development. *Sci. Transl. Med.* **2013**, *5*, 204ra132.

(17) Baym, M.; Stone, L. K.; Kishony, R. Multidrug Evolutionary Strategies to Reverse Antibiotic Resistance. *Science* **2016**, *351*, aad3292.

(18) Nichol, D.; Rutter, J.; Bryant, C.; Hujer, A.; Lek, S.; Adams, M.; Jeavons, P.; Anderson, A.; Bonomo, R.; Scott, J. G. Antibiotic Collateral Sensitivity Is Contingent on the Repeatability of Evolution. *Nat. Commun.* **2019**, *10*, 334.

(19) Beckley, A. M.; Wright, E. S. Identification of Antibiotic Pairs That Evade Concurrent Resistance via a Retrospective Analysis of Antimicrobial Susceptibility Test Results. *Lancet Microbe* **2021**, *2*, e545–e554.

(20) Brepoels, P.; Appermans, K.; Pérez, C. A.; Lories, B.; Marchal, K.; Steenackers, H. Antibiotic Cycling Affects Resistance Evolution Independently of Collateral Sensitivity. *Mol. Biol. Evol.* **2022**, *39*, msac257.

(21) Barbosa, C.; Römhild, R.; Rosenstiel, P.; Schulenburg, H. Evolutionary Stability of Collateral Sensitivity to Antibiotics in the Model Pathogen *Pseudomonas Aeruginosa*. *eLife* **2019**, *8*, No. e51481.

(22) Ghaddar, N.; Hashemidahaj, M.; Findlay, B. L. Access to High-Impact Mutations Constrains the Evolution of Antibiotic Resistance in Soft Agar. *Sci. Rep.* **2018**, *8*, 17023.

(23) Langevin, A. M.; El Meouche, I.; Dunlop, M. J. Mapping the Role of AcrAB-TolC Efflux Pumps in the Evolution of Antibiotic Resistance Reveals Near-MIC Treatments Facilitate Resistance Acquisition. *mSphere* **2020**, *5*, 010566.

(24) Sulavik, M. C.; Gambino, L. F.; Miller, P. F. The MarR Repressor of the Multiple Antibiotic Resistance (Mar) Operon in *Escherichia Coli*: Prototypic Member of a Family of Bacterial Regulatory Proteins Involved in Sensing Phenolic Compounds. *Mol. Med.* **1995**, *1*, 436–446.

(25) Zhang, H.; Ma, Y.; Liu, P.; Li, X. Multidrug Resistance Operon EmrAB Contributes for Chromate and Ampicillin Co-Resistance in a *Staphylococcus* Strain Isolated from Refinery Polluted River Bank. *SpringerPlus* **2016**, *5*, 1648.

(26) Ariza, R. R.; Li, Z.; Ringstad, N.; Demple, B. Activation of Multiple Antibiotic Resistance and Binding of Stress-Inducible Promoters by *Escherichia Coli* Rob Protein. *J. Bacteriol.* **1995**, *177*, 1655–1661.

(27) Soto, S. M. Role of Efflux Pumps in the Antibiotic Resistance of Bacteria Embedded in a Biofilm. *Virulence* **2013**, *4*, 223–229.

(28) Nishino, K.; Yamasaki, S.; Nakashima, R.; Zwama, M.; Hayashi-Nishino, M. Function and Inhibitory Mechanisms of Multidrug Efflux Pumps. *Front. Microbiol.* **2021**, *12*, 12.

(29) Nikaido, H. Antibiotic Resistance Caused by Gram-Negative Multidrug Efflux Pumps. *Clin. Infect. Dis.* **1998**, *27*, S32–S41.

(30) Dunai, A.; Spohn, R.; Farkas, Z.; Lázár, V.; Györkei, Á.; Apjok, G.; Boross, G.; Szappanos, B.; Grézal, G.; Faragó, A.; Bodai, L.; Papp, B.; Pál, C. Rapid Decline of Bacterial Drug-Resistance in an Antibiotic-Free Environment through Phenotypic Reversion. *eLife* **2019**, *8*, No. e47088.

(31) Anes, J.; McCusker, M. P.; Fanning, S.; Martins, M. The Ins and Outs of RND Efflux Pumps in *Escherichia Coli*. *Front. Microbiol.* **2015**, *6*, 587.

(32) Olivares Pacheco, J.; Alvarez-Ortega, C.; Alcalde Rico, M.; Martínez, J. L. Metabolic Compensation of Fitness Costs Is a General Outcome for Antibiotic-Resistant *Pseudomonas Aeruginosa* Mutants Overexpressing Efflux Pumps. *mBio* **2017**, *8*, No. e00500.

(33) Juhas, M.; Ajioka, J. W. Identification and Validation of Novel Chromosomal Integration and Expression Loci in *Escherichia Coli* Flagellar Region 1. *PLoS One* **2015**, *10*, No. e0123007.

(34) Khamari, B.; Adak, S.; Chanakya, P. P.; Lama, M.; Peketi, A. S. K.; Gurung, S. A.; Chettri, S.; Kumar, P.; Bulagonda, E. P. Prediction

of Nitrofurantoin Resistance among Enterobacteriaceae and Mutational Landscape of in Vitro Selected Resistant *Escherichia Coli*. *Res. Microbiol.* **2022**, *173*, 103889.

(35) Roemhild, R.; Linkevicius, M.; Andersson, D. I. Molecular Mechanisms of Collateral Sensitivity to the Antibiotic Nitrofurantoin. *PLoS Biol.* **2020**, *18*, No. e3000612.

(36) Gerrish, P. J.; Lenski, R. E. The Fate of Competing Beneficial Mutations in an Asexual Population. *Genetica* **1998**, *102/103*, 127–144.

(37) Łapińska, U.; Voliotis, M.; Lee, K. K.; Campey, A.; Stone, M. R. L.; Tuck, B.; Phetsang, W.; Zhang, B.; Tsaneva-Atanasova, K.; Blaskovich, M. A.; Pagliara, S. Fast Bacterial Growth Reduces Antibiotic Accumulation and Efficacy. *eLife* **2022**, *11*, No. e74062.

(38) Roemhild, R.; Andersson, D. I. Mechanisms and Therapeutic Potential of Collateral Sensitivity to Antibiotics. *PLoS Pathog.* **2021**, *17*, No. e1009172.

(39) Tao, K.; Watanabe, S.; Narita, S.; Tokuda, H. A Periplasmic LolA Derivative with a Lethal Disulfide Bond Activates the Cpx Stress Response System. *J. Bacteriol.* **2010**, *192*, 5657–5662.

(40) Choi, U.; Lee, C.-R. Distinct Roles of Outer Membrane Porins in Antibiotic Resistance and Membrane Integrity in *Escherichia Coli*. *Front. Microbiol.* **2019**, *10*, 953.

(41) Tajima, T.; Yokota, N.; Matsuyama, S.; Tokuda, H. Genetic Analyses of the in Vivo Function of LolA, a Periplasmic Chaperone Involved in the Outer Membrane Localization of *Escherichia Coli* Lipoproteins. *FEBS Lett.* **1998**, *439*, 51–54.

(42) Pelchovich, G.; Schreiber, R.; Zhuravlev, A.; Gophna, U. The Contribution of Common RpsL Mutations in *Escherichia Coli* to Sensitivity to Ribosome Targeting Antibiotics. *Int. J. Med. Microbiol.* **2013**, *303*, 558–562.

(43) Sandegren, L.; Andersson, D. I. Bacterial Gene Amplification: Implications for the Evolution of Antibiotic Resistance. *Nat. Rev. Microbiol.* **2009**, *7*, 578–588.

(44) Hjort, K.; Nicoloff, H.; Andersson, D. I. Unstable Tandem Gene Amplification Generates Heteroresistance (Variation in Resistance within a Population) to Colistin in *Salmonella Enterica*. *Mol. Microbiol.* **2016**, *102*, 274–289.

(45) Greulich, P.; Scott, M.; Evans, M. R.; Allen, R. J. Growth-Dependent Bacterial Susceptibility to Ribosome-Targeting Antibiotics. *Mol. Syst. Biol.* **2015**, *11*, 0796.

(46) Jagielski, T.; Ignatowska, H.; Bakula, Z.; Dziewit, Ł.; Napiórkowska, A.; Augustynowicz-Kopeć, E.; Zwolska, Z.; Bielecki, J. Screening for Streptomycin Resistance-Confering Mutations in *Mycobacterium Tuberculosis* Clinical Isolates from Poland. *PLoS One* **2014**, *9*, No. e100078.

(47) Melchionna, M. V.; Gullett, J. M.; Bouveret, E.; Shrestha, H. K.; Abraham, P. E.; Hettich, R. L.; Alexandre, G. Bacterial Homologs of Progesterin and AdipoQ Receptors (PAQRs) Affect Membrane Energetics Homeostasis but Not Fluidity. *J. Bacteriol.* **2022**, *204*, No. e0058321.

(48) Bruni, G. N.; Kralj, J. M. Membrane Voltage Dysregulation Driven by Metabolic Dysfunction Underlies Bactericidal Activity of Aminoglycosides. *eLife* **2020**, *9*, No. e58706.

(49) Xing, Y.; Kang, X.; Zhang, S.; Men, Y. Specific Phenotypic, Genomic, and Fitness Evolutionary Trajectories toward Streptomycin Resistance Induced by Pesticide Co-Stressors in *Escherichia Coli*. *ISME Commun.* **2021**, *1*, 39.

(50) Zogaj, X.; Nimtz, M.; Rohde, M.; Bokranz, W.; Römling, U. The Multicellular Morphotypes of *Salmonella Typhimurium* and *Escherichia Coli* Produce Cellulose as the Second Component of the Extracellular Matrix. *Mol. Microbiol.* **2001**, *39*, 1452–1463.

(51) Serra, D. O.; Richter, A. M.; Hengge, R. Cellulose as an Architectural Element in Spatially Structured *Escherichia Coli* Biofilms. *J. Bacteriol.* **2013**, *195*, 5540–5554.

(52) Reizer, J.; Reizer, A.; Saier, M. H. Novel Phosphotransferase System Genes Revealed by Bacterial Genome Analysis—a Gene Cluster Encoding a Unique Enzyme I and the Proteins of a Fructose-like Permease System. *Microbiology* **1995**, *141*, 961–971.

- (53) Zelcbuch, L.; Lindner, S. N.; Zegman, Y.; Vainberg Slutskin, I.; Antonovsky, N.; Gleizer, S.; Milo, R.; Bar-Even, A. Pyruvate Formate-Lyase Enables Efficient Growth of *Escherichia Coli* on Acetate and Formate. *Biochemistry* **2016**, *55*, 2423–2426.
- (54) Criswell, D.; Tobiasson, V. L.; Lodmell, J. S.; Samuels, D. S. Mutations Conferring Aminoglycoside and Spectinomycin Resistance in *Borrelia Burgdorferi*. *Antimicrob. Agents Chemother.* **2006**, *50*, 445–452.
- (55) Kenney, T. J.; Churchward, G. Cloning and Sequence Analysis of the RpsL and RpsG Genes of *Mycobacterium Smegmatis* and Characterization of Mutations Causing Resistance to Streptomycin. *J. Bacteriol.* **1994**, *176*, 6153–6156.
- (56) Hernando-Amado, S.; Laborda, P.; Valverde, J. R.; Martínez, J. L. Rapid Decline of Ceftazidime Resistance in Antibiotic-Free and Sublethal Environments Is Contingent on Genetic Background. *Mol. Biol. Evol.* **2022**, *39*, msac049.
- (57) Hibbing, M. E.; Fuqua, C.; Parsek, M. R.; Peterson, S. B. Bacterial Competition: Surviving and Thriving in the Microbial Jungle. *Nat. Rev. Microbiol.* **2010**, *8*, 15–25.
- (58) Pao, S. S.; Paulsen, I. T.; Saier, M. H. Major Facilitator Superfamily. *Microbiol. Mol. Biol. Rev.* **1998**, *62*, 1–34.
- (59) Daley, D. O.; Rapp, M.; Granseth, E.; Melén, K.; Drew, D.; von Heijne, G. Global Topology Analysis of the *Escherichia Coli* Inner Membrane Proteome. *Science* **2005**, *308*, 1321–1323.
- (60) Dassler, T.; Maier, T.; Winterhalter, C.; Böck, A. Identification of a Major Facilitator Protein from *Escherichia Coli* Involved in Efflux of Metabolites of the Cysteine Pathway. *Mol. Microbiol.* **2000**, *36*, 1101–1112.
- (61) Saier, M. H.; Reddy, V. S.; Tsu, B. V.; Ahmed, M. S.; Li, C.; Moreno-Hagelsieb, G. The Transporter Classification Database (TCDB): Recent Advances. *Nucleic Acids Res.* **2016**, *44*, D372–379.
- (62) Wang, H.; Yin, X.; Wu Orr, M.; Dambach, M.; Curtis, R.; Storz, G. Increasing Intracellular Magnesium Levels with the 31-Amino Acid MgtS Protein. *Proc. Natl. Acad. Sci. U.S.A.* **2017**, *114*, 5689–5694.
- (63) Weaver, J.; Mohammad, F.; Buskirk, A. R.; Storz, G. Identifying Small Proteins by Ribosome Profiling with Stalled Initiation Complexes. *mBio* **2019**, *10*, 028199.
- (64) Lee, H.-J.; Gottesman, S. SRNA Roles in Regulating Transcriptional Regulators: Lrp and SoxS Regulation by SRNAs. *Nucleic Acids Res.* **2016**, *44*, 6907–6923.
- (65) Jonas, K.; Edwards, A. N.; Simm, R.; Romeo, T.; Römling, U.; Melefors, O. The RNA Binding Protein CsrA Controls Cyclic Di-GMP Metabolism by Directly Regulating the Expression of GGDEF Proteins. *Mol. Microbiol.* **2008**, *70*, 236–257.
- (66) Sandegren, L.; Lindqvist, A.; Kahlmeter, G.; Andersson, D. I. Nitrofurantoin Resistance Mechanism and Fitness Cost in *Escherichia Coli*. *J. Antimicrob. Chemother.* **2008**, *62*, 495–503.
- (67) Sargentini, N. J.; Gularte, N. P.; Hudman, D. A. Screen for Genes Involved in Radiation Survival of *Escherichia Coli* and Construction of a Reference Database. *Mutat. Res.* **2016**, *793–794*, 1–14.
- (68) Amundsen, S. K.; Taylor, A. F.; Chaudhury, A. M.; Smith, G. R. recD: the gene for an essential third subunit of exonuclease V. *Proc. Natl. Acad. Sci. U.S.A.* **1986**, *83*, 5558–5562.
- (69) Frenoy, A.; Bonhoeffer, S. Death and Population Dynamics Affect Mutation Rate Estimates and Evolvability under Stress in Bacteria. *PLoS Biol.* **2018**, *16*, No. e2005056.
- (70) Loftie-Eaton, W.; Bashford, K.; Quinn, H.; Dong, K.; Millstein, J.; Hunter, S.; Thomason, M. K.; Merrikk, H.; Ponciano, J. M.; Top, E. M. Compensatory Mutations Improve General Permissiveness to Antibiotic Resistance Plasmids. *Nat. Ecol. Evol.* **2017**, *1*, 1354–1363.
- (71) Szamecz, B.; Boross, G.; Kalapis, D.; Kovács, K.; Fekete, G.; Farkas, Z.; Lázár, V.; Hrtyan, M.; Kemmeren, P.; Groot Koerkamp, M. J. A.; Rutkai, E.; Holstege, F. C. P.; Papp, B.; Pál, C. The Genomic Landscape of Compensatory Evolution. *PLoS Biol.* **2014**, *12*, No. e1001935.
- (72) Sanz-García, F.; Gil-Gil, T.; Laborda, P.; Blanco, P.; Ochoa-Sánchez, L.-E.; Baquero, F.; Martínez, J. L.; Hernando-Amado, S. Translating Eco-Evolutionary Biology into Therapy to Tackle Antibiotic Resistance. *Nat. Rev. Microbiol.* **2023**, 1–15.
- (73) Ocampo, P. S.; Lázár, V.; Papp, B.; Arnoldini, M.; Abel zur Wiesch, P.; Busa-Fekete, R.; Fekete, G.; Pál, C.; Ackermann, M.; Bonhoeffer, S. Antagonism between Bacteriostatic and Bactericidal Antibiotics Is Prevalent. *Antimicrob. Agents Chemother.* **2014**, *58*, 4573–4582.
- (74) Batra, A.; Roemhild, R.; Rousseau, E.; Franzenburg, S.; Niemann, S.; Schulenburg, H. High Potency of Sequential Therapy with Only  $\beta$ -Lactam Antibiotics. *eLife* **2021**, *10*, No. e68876.
- (75) Amor, D. R.; Gore, J. Fast Growth Can Counteract Antibiotic Susceptibility in Shaping Microbial Community Resilience to Antibiotics. *Proc. Natl. Acad. Sci. U.S.A.* **2022**, *119*, No. e2116954119.
- (76) Melnyk, A. H.; McCloskey, N.; Hinz, A. J.; Dettman, J.; Kassen, R. Evolution of Cost-Free Resistance under Fluctuating Drug Selection in *Pseudomonas Aeruginosa*. *mSphere* **2017**, *2*, 001588.
- (77) Brewster, J. D. A simple micro-growth assay for enumerating bacteria. *J. Microbiol. Methods* **2003**, *53*, 77–86.
- (78) Sprouffske, K.; Wagner, A. Growthcurver: an R package for obtaining interpretable metrics from microbial growth curves. *BMC Bioinf.* **2016**, *17*, 172.
- (79) CLSI, M07: Dilution AST for Aerobically Grown Bacteria; CLSI. <https://clsi.org/standards/products/microbiology/documents/m07/> (accessed 12 Jan, 2020).
- (80) Deatherage, D. E.; Barrick, J. E. Identification of Mutations in Laboratory-Evolved Microbes from next-Generation Sequencing Data Using Breseq. *Methods Mol. Biol.* **2014**, *1151*, 165–188.